A VOLTAMMETRY STUDY OF ETHANOL OXIDATION ON CARBON SUPPORTED PLATINUM - TUNGSTEN CATALYSTS

R. Hernández[1], Orlando Ugalde Reyes [1], H. Castañeda [2],
Jesús Gracia Fadrique [1], Pedro Roquero Tejeda [1,*]

[1] Facultad de Química, Universidad Nacional Autónoma de México. Avenida Universidad 3000, Coyoacán, 04510 México D.F.

[2] Battelle Memorial Institute, Energy Systems, 505 King Avenue, Columbus OH 43201, USA

ABSTRACT

This paper presents the results of the synthesis and characterization of bimetallic catalysts with Pt and W as active phases, supported on XC72R carbon. A synthesis method based on the thermolysis of metal precursors was used, in systems in which an aqueous phase, an organic one (dichlorobenzene) and solid carbon was present. The Pt loading in the synthesized catalysts was kept constant, and the amounts of W and graphite were changed. The physical characterization was performed using transmission electron microscopy. It was found that the Pt phase form hemispherical particles with average diameter of 3 nm. The W is predominantly in the form of hexagonal WO_3, forming crystals with average dimensions 35 by 15 nm. No evidence of alloy formation is found. The electrochemical characterization of ethanol oxidation includes cyclic voltammetry and current–sampled voltammetry techniques. It was found that tungsten exerts a clear promoting role in the activity of the catalysts, revealed by considerably increased current densities with respect to carbon – supported Pt. Some details of this enhanced activity are revealed by cyclic voltammetry experiments with different operating conditions and electrolyte formulations. This allowed to identify the oxidation of adsorbed organic intermediates influenced by the tungsten phase. WO_3 appears as well to cause the decrease in the rate at which Pt oxides reduce, leading to higher surface coverage of $OH^{\bullet}$ species.

Keywords: *Anodic Ethanol Oxidation, Voltammetry, Platinum, Tungsten, Fuel Cell Catalyst*.

* Corresponding author, roquero@unam.mx

1. Introduction

In recent years, the use of fossil fuels, especially oil and gas, has accelerated the concern about a global energy crisis. Major efforts will focus on finding methods of producing electricity efficiently and with the least possible environmental impact. The new electricity has to come from renewable energy sources. Fuel cells, that are a promising option for energy conversion, are based on an electrochemical principle which continuously converts chemical energy into electrical energy, accompanied by heat, for a variety of fuels and oxidizers. [1-5] Ethanol is a hydrogen-carrier molecule that has been pronounced as a strong candidate to replace methanol in this kind of device, mainly because of its high energy density and low permeability in polymeric proton-conducting membranes. Another advantage of ethanol is that it is not harmful to humans, unlike methanol, and can be directly produced from biomass [6-12].

The total conversion of ethanol to CO_2 is the central issue in the performance of electrocatalysts in direct ethanol fuel cells. The complete oxidation of ethanol involves the cleavage of a C-C bond and the formation of CO bonds that lead to the formation of carbon dioxide. The efficiency of C-C bond activation in the oxidation of ethanol is the key to the possible application of this reaction in fuel cells. [6, 9-12] Several investigations have focused on the catalysts formulations. Pt is susceptible to the adsorption of CO species and other reaction intermediates. Bimetallic and trimetallic have been used to increase catalytic activity and to avoid poisoning by CO molecules or other intermediates [10-13]. Among the most studied bimetallic catalysts are Pt-Ru / C [7, 11, 13, 14]; Pt-Sn / C [10, 15]; Pt-Rh / C [6, 10, 13]; Pt-Mo / C [14]. Trimetallic catalysts have also been tested, mainly Pt-Rh-SnO_2 / C [10]; PtRuMo / C [11] and Pt-Ru -Rh [13].

The anodic oxidation of ethanol involves the formation of different intermediates that can have one or two carbon atoms. The complete reaction to yield CO_2 requires the cleavage of the C-C bond and the addition of three oxygen atoms to the original fuel molecule. Several studies present evidence of the formation of C_1 intermediates: CH_x and CO [16, 17]. While other works report the presence of adsobed C_2 intermediates at the Pt surface [18, 19]. Both

types of intermediate can coexist and their relative predominance is a function of electrode potential [20]. It has been also demonstrated that the selectivity towards the C_2 intermediates is increased at smooth Pt surfaces, and the C-C bond breaking is favored at stepped surfaces [21].

Scheme 1 represents possible reaction routes of ethanol oxidation, considering only stable C_2 intermediates and omitting gem-diols (which could only be formed by direct oxidation of acetaldehyde or ethyleneglycol, without deprotonation). Other intermediates may exist, stabilized by the interaction with Pt. The dehydrogenation is a two-electron process, while oxygen addition is a one-electron reaction. Also, the dissociation of three water molecules per ethanol molecule, forming OH• species, is required for the complete oxidation. Considering the acetate and acetyl ions as the only C_2 intermediates experimentally found [ref], this latter suggests that once each carbon atom bears one oxygen atom, the C-C splitting is facilitated and C_1 intermediates become predominant. The possible reaction paths for these C_1 intermediates are presented in scheme 2. Partial surface coverage by CH_x adsorbates has been determined by in-situ spectroscopic techniques [16]. The presence of these intermediates can only be found in catalysts in which C-C bond cleavage is easy to accomplish.

The formulation of fuel cell catalysts with different tungsten promoting phases has been studied by several groups with promising results as a CO tolerant anode in the oxidation of ethanol and methanol [22-26]. While in Pt-Ru and Pt-Sn catalysts the activity enhancement is attributed to a combination of the bifunctional mechanism and the ligand effect, in the case of some tungsten-containing catalysts it has also been proposed that a hydrogen spillover effect may occur, continuously cleaning the platinum surface [27]. However, it is still not clear how this effect can play a role in the rate-determining step at the electrode potentials in which alcohol oxidation takes place.

In this work the electrochemical behavior of carbon supported Pt-W catalysts was studied by means of cyclic voltammetry and current-sampled voltammetry, with different ethanol concentrations. The catalysts synthesis method produces materials with separate Pt and

WO_3 phases, as revealed by HRTEM and XRD. There is no evidence of alliages formed between both metals. No significative changes were found in the oxidation potentials in the W-containing materials with respect to Pt, but electrical currents are considerably enhanced by the presence of WO_3. Cyclic voltammetry results reveal the existence of adsorbed organic intermediates, at high electrode potentials, that are oxidized easily in the presence of tungsten.

2. Experimental procedure

2.1 Catalysts synthesis

Ordóñez et. al. [28] proposed the synthesis of Pt-W/C catalysts. Similar methodology is used for Pt carbonyl complex, tugnsten hexacarbonyl complex ($W(CO)_6$) and Vulcan XC72R carbon in a reflux system and dichlorobenzene as solvent.

The Pt hexacarbonyl complex was synthesized by bubbling CO during 24 h at a volumetric flow rate of 25 cm^3/min through 50 ml of an aqueous chloroplatinic acid solution (10mg/cm^3 H_2PtCl_6) [29]. With the materials in the glass container, the system temperature was increased up to the boiling point of dichlorobenzene, (120 ºC) and reflux was maintained for 24 h. Once this contact time was reached, the solvent was distilled, the precipitate was filtered, washed first with diethyl ether and then with bidistillated water. The materials were then subjected to thermal treatment under N_2 atmosphere at 400 ºC during 4 hours. Compositions of the prepared catalysts are presented in table 1.

2.2 Catalysts characterization

The working electrodes were prepared by mixing 1 mg of each catalyst, 10 μL of 5 % Nafion solution, 10 μL of 2-propanol. The mixture was ultrasonically suspended to obtain slurry paste. 5 μL of this slurry was placed on the surface of a 0.19 cm^2 glassy carbon electrode forming a thin layer. A 0.5 M H_2SO_4 solution was used as supporting electrolyte. Working solutions contained 0.5, 1, 1.5 and 2 M ethanol in addition to the sulfuric acid. The solutions were purged with N_2 during 15 minutes before testing. The electrochemical

experiments were conducted at 25 ºC, using a Radiometer Voltalab 50 potentiostat-galvanostat. A three-electrode cell was used with saturated calomel electrode (SCE) as reference and graphite electrode as counter-electrode.

The current obtained for the half cell experiments during ethanol oxidation were normalized. , and obtained by stripping voltammetry of a CO monolayer. By assuming: no CO adsorption occurs on tungsten phases and that the oxidation of this monolayer requires 420 $\mu C/cm^2$ [30,31]. The working electrode potential was fixed at 100 mV vs. SCE during 1 h in a CO saturated 0.5 M H_2SO_4 solution. This electrolyte was replaced by a CO – free, sulfuric acid solution and CV tests were carried out between -300 at 1400 mV vs SCE at a scan rate of 10 mV s^{-1}.

Open circuit potentials (OCP) were measured during 1 hour. The cyclic voltammmetry measurements started at the OCP value and all sweeps were first carried out towards negative potentials and then reversed towards positive potentials. The potential window was from-0.3 to 1.4 V *vs* SCE in ethanol solutions and three kinds of voltammetry experiment were performed: 1) Potential sweeps in varying ethanol concentration electrolytes; 2) Potential sweeps with varying scan rate (50, 100, 250, 500, 1000 mV s^{-1}) and 3) Current-sampled voltammetry at a rotating disk electrode with a 1500 rpm speed, between 0.2 at 1.35 V vs SCE. The application of potential steps included 5 mV and the recording of steady state current 60 s after the potential step.

Samples used for Transmission Electron Microscopy were dispersed in n-heptane, in an ultrasound bath for 1 h. Some drops of the supernatant liquid were deposited on 200-mesh copper grids covered with a carbon film and images were obtained with a JEOL 2010 microscope.

3. Results and Discussion

Normalized active areas of the catalysts were calculated using the results from the CO stripping voltammetry. Figure 1 illustrates the CO oxidation peaks at potential between

0.35 and 0.65 V. Also, the figure represents the completely oxidized CO to CO_2 during the first sweep potential. The second scan was used as the baseline for calculating the active area. The results are summarized in Table 2. In these tests the increment in the W causes a decrease in the Pt active surface. Voltammograms show the $Pt_{50}W_{50}$/C and $Pt_{67}W_{33}$/C similar electrical charges in the CO oxidation step, but the peak in $Pt_{50}W_{50}$/C is shifted to a higher potential with respect to the other materials, indicating that in this catalyst CO adsorption is stronger than in the others.

Figure 2(A) displays the voltammograms of the prepared catalysts Pt_{20}/C_{80}, $Pt_{80}W_{20}$/C, $Pt_{67}W_{33}$/ C and $Pt_{50}W_{50}$/C in 0.5 M H_2SO_4. Potential scans start at the OCP value, close to 0.53 V vs. SCE in all cases, and sweeps starting the negative potential up to 0.3 V vs. SCE, and the returning to positive potentials. These currents are characteristic of platinum resulting from hydrogen dissociative adsorption (I) and proton desorption (II) at Pt (111), Pt (110) and Pt (100) surfaces [32,33]. Peak III is related to the Pt oxidation to form $Pt(OH)_2$ and PtO, preceding the oxygen discharge. When the scan is reversed towards negative potentials, peak IV appears, corresponding to the reduction of Pt oxides. The presence of tungsten in these materials seems to enhance the electrochemical activity of Pt but no redox process that could be attributed to W can be identified. Figure 2(B) presents the catalytic behavior of W_{20}/C_{80} in the electrolyte support and differente ethanol concentrations. There are no changes occur in the voltammetry response in 0.5 M of H_2SO_4 solution, in the absence and presence of ethanol. It can be concluded that the W/C material does not exhibit any appreciable electrocatalytic behavior towards ethanol oxidation. These results are consistent with those obtained by Maillard et. al. for a carbon-supported Pt-WO_x catalyst in 1 M H_2SO_4 [24], and Bozzini et. al. in a bare WC electrode immersed in 0.1 M $HClO_4$, in the absence and presence of ethanol [34].

Figure 3 shows the oxidation of ethanol, at different concentrations, on the surface of all tested Pt catalysts. Peaks V and VI in the positive scan are due to the ethanol adsorption and initial oxidation steps (depicted at the left side of scheme 1). In the reverse scan, the anodic peaks VII and VIII are due to the oxidation of adsorbed intermediates that react with OH• produced at high potentials, either from Pt or W oxides (right side in scheme 1 and

scheme 2). These anodic peaks have been identified as *renewed oxidation* by some authors [35]. In previous works the availability of oxygen reactive species, obtained from the water dissociation, is crucial in the complete oxidation of ethanol and thus, in the efficiency of fuel cell catalysts [36]. This is the reason why peaks VII and VIII are the most important to be considered in the characterization of catalysts for anodes in direct alcohol fuel cells. The onset potential of the oxidation reaction has a different behavior as a function of the ethanol concentration. In the case presented in figure 3(A), at a 0.5 M ethanol concentration, the catalyst Pt_{20}/C_{80} presents an onset potential of 0.15 V vs. SCE, while catalysts $Pt_{80}W_{20}/C$ and $Pt_{67}W_{33}/C$ display onset potentials at about 0.050 V. For the catalyst $Pt_{50}W_{50}/C$, the onset potential is 0.15 V. In figure 3(B), the catalyst Pt_{20}/C_{80} presents an onset potential of 0.1 V, while catalysts $Pt_{80}W_{20}/C$ and $Pt_{67}W_{33}/C$ show an onset potential of 0.060 V, and catalyst $Pt_{50}W_{50}/C$ an onset potential of 0.12 V. In figure 3(C) we can appreciate that all catalysts tested showed an onset potential of 0.1 V. The highest anodic currents are found, in all cases, with the $Pt_{67}W_{33}/C$ catalyst. It is clear that the presence of tungsten improves the catalytic activity of Pt to oxidize ethanol. Similarly, with increasing concentration of ethanol, the amount of current generated in each oxidation peak increases, this effect can be associated to the saturation of active sites at the surface of electrode [33] and leads predominantly to a reaction scheme based in C_2 intermediates (scheme 1).

Figure 4 resumes the peak potentials and the corresponding electrical charges as a function of ethanol concentration for all the tests carried out. The onset potential of the ethanol oxidation reaction showed a tendency to be lower for catalysts with W in its formulation, the potential of peaks V and VI first increases with ethanol concentration and then decrease at high fuel concentration (Figure 4A and C) and a similar behavior follows the electrical charge for the $Pt_{80}W_{20}/C$ catalyst. Different samples materials resulted in the electrical charge increment with ethanol concentration (Figure 4B and D). This indicates that, although Pt active sites may become saturated at high ethanol concentrations, the reaction rate is increased by the addition of W to the materials. In the case of peak VII, obtained in the reverse scan of each voltammetry, both, the potential and charge increase as a function of ethanol concentration and are considerably higher in the W-containing materials that in the reference Pt_{20}/C_{80}.

Figure 5 illustrates the voltammograms obtained from reverse sweeps at low and high scan rates (50 to 1000 mV s^{-1}). The peak for Pt_{20}/C_{80} (figure 5A) is visible, but there is no signal of peak VII. As scan-rate is increased, the current of this peak becomes larger and its potential shifts to more negative potentials, but when scan rate is 500 mV s^{-1} or higher a cathodic current is observed and the anodic current of peak VIII decreases. This is attributed to the high scan rates Pt oxides undergo rapid reduction and do not participate in the renewed oxidation process, decreasing thus the anodic current of peak VIII. By applying high scan rates, the capacitive currents become important and the analysis of the electrical charge can no longer be attributed only to oxidation or reduction reactions. The catalysts formulated with tungsten present all the peak VII (figure 5B,C,D), that cannot be seen in Pt_{20}/C_{80}. This suggests that, in this potential range, W is facilitating the oxidation of adsorbed intermediates. In $Pt_{80}W_{20}/C$ and $Pt_{50}W_{50}/C$, (Figure 5B and D) a small shoulder preceding peak VII can be appreciated. Further work is required to identify the nature of the intermediates involved in this process.

Experiments with low-scan rates were performed in order to better understand the appearance of oxidation processes in electrolytes containing organic molecules. Figure 6 demostrates the CV results for two catalysts: Pt_{20}/C_{80} and $Pt_{50}W_{50}/C$. In the case of Pt_{20}/C_{80}, in the scan towards positive potentials (figure 6A) peaks V and VI are clearly defined and shift slightly to positive potentials as the scan rate is increased. In the reverse sweep (figure 6A') peak VII is visible, which was not the case of high scan rates (figure 5). Peak VIII is sharper as rate is increased and its potential does not considerably change. This confirms that the anodic current in this stage is due to oxidation of adsorbed intermediates. $Pt_{50}W_{50}/C$ (figure 6 B) voltammogram shows, the same overall behavior as in the previous case, but the shoulder that precedes peak VII is now clearly defined and it shifts to higher potentials as the scan rate is increased. This effect can only be attributed to an increasing oxidation activity of the catalyst originated from the interaction of W phases with adsorbed intermediates in the potential range 0.55 to 0.8 V vs. SCE that, to our knowledge, has not been reported previously.

Figure 7 provides steady-state currents as a function of the applied potential, and is a better representation of the performance of a catalyst in real fuel cell operation conditions, than cyclic voltammetry. Cell stirring ensures that mass-transport limitations are minimized and current sampling reduces the effects of capacitive charging at the electrical double layerThe results displayed the behavior of current density similar to that observed in cyclic voltammetry: there are two current peaks for each ethanol concentration tested. In the case of 0.5 and 1 M of ethanol, the maximum current is obtained in the $Pt_{67}W_{33}/C$ catalyst, but when the concentration is 1.5 M ethanol, the maximum current is given by the $Pt_{50}W_{50}/C$ catalyst. In all cases there is a significant increase in the current response when the W is present in the catalysts. It is to be noted that for the first peak, corresponding to peak V in cyclic voltammetry, for the 1.5 M ethanol electrolyte, a difference of 0.1 V is found between the CV and the steady-state results. In the case of the second peak, corresponding to the peak VI of cyclic voltammetry, the difference in peak potential between both techniques is about 0.05 V at all concentrations.

In figure 8 are shown the HRTEM images of three materials: the two single metal materials and the catalyst with equal loadings of both metals. polycrystalline Pt with mean particle diameter of 3 nm are found in Pt_{20}/C_{80}. this active phase is well dispersed on carbon particles with diameter around 40 nm (figure 8A). In W_{20}/C_{80} hexagonal WO_3 is the predominant phase, forming crystallites of average dimension 35 by 15 nm. From figure 8C it can be seen that the bimetallic catalyst $Pt_{50}W_{50}/C$ is made up of the same phases as the single-metal materials. No alloying of Pt and W has been found and the interatomic distances measured in Pt and WO_3 particles remain the same and the promoting effect of tungsten in the catalytic activity should be related to interaction phenomena between particles of the carbon support and the active phases.

4. Conclusions

A complete voltammetry study of ethanol oxidation on platinum – tungsten, supported catalysts has been performed. The selected synthesis method leads to materials in which the active phases, Pt and WO_3, coexist in the surface of the support without forming alloys, as

confirmed by HRTEM analysis. The use of simple DC potentiodynamic and potentiostatic techniques in half-cell configuration provided important information on the behavior of these materials and revealed its viability to be used as anode catalysts in direct alcohol fuel cells. Onset and peak potentials of the ethanol oxidation are not considerably different in the W – containing catalysts in comparison with the supported Pt material, but anodic currents are considerably and consistently higher when W is present in the formulation, despite the fact that its presence leads to a decrease in Pt effective surface area.

By varying ethanol concentration in the electrolyte and scan rate, it was possible to identify the oxidation of intermediates that had not been previously reported, and their apparent interaction with WO_3 during charge-transfer reactions. The promoting effect of tungsten can be related to the bifunctional mechanism proposal, as it takes place at potentials that correspond to water decomposition, but this does not fully explain the observed behavior: since Pt and W are not intimately related in these catalysts, a surface spillover effect may be partly responsible for the voltammetry response, and might be influencing the overall electronic structure of the solid.

An interesting result is related to the fact that, at high potential scan rates, the renewed oxidation of adsorbed intermediates is partially suppressed as Pt oxides reduce without receiving electrons from the mentioned intermediates, but the presence of tungsten does eliminate this effect, perhaps by decreasing the reduction rate of Pt oxides and allowing that these species participate in the oxidation process.

Further work is required to identify the involved intermediates that can be adsorbed at different surfaces in the catalysts. In-situ spectroscopic techniques and on-line mass spectrometry, in half-cell and membrane-electrode assemblies, will be applied in the continuation of this study. Identification of surface active sites and related organic intermediates should allow to improve the design of these, and other catalysts in fuel cell applications.

Acknowledgements

The authors thank Mr. Ivan Puente Lee for the obtention of TEM images. R. Hernández and O. Ugalde thank Conacyt-México the PhD grants and financial support for this work.

References

[1] L. Carrette, K. A. Friedrich and U. Stimming. *Fuel Cells: Fundamentals and Applications*, Fuel Cells, 1, 1, 5, 2001.

[2] G. Hoogers. *Fuel Cell Technology Handbook*. CRC Press LLC, New York, 2003.

[3] EG&G Technical Services, Inc. Science Applications International Corporation. *Fuel Cell Handbook*, West Virginia, 2002.

[4] M. Schulze, N. Wagner, T. Kaz, K. A. Friedrich.. *Electrochim Acta*, 52, 2328, 2007.

[5] F. Vigier, S. Rousseau, C. Coutanceau, J. M. Leger and C. Lamy. *Topics in Catal*, 40, 1-4, 111, 2006.

[6] K. Bergamaski, E. R. Gonzales, F. C. Nart. *Electrochim Acta*. 53, 4396, 2008.

[7] K. Taneda, Y. Yamazaki. *Electrochim Acta*, 52, 1627, 2006.

[8] Y. S. Li, T. S. Zhao, Z. X, Liang. *J. Power Sources*, 187, 387, 2009.

[9] V. Bambagioni, C. Bianchini, A. Marchionni, J. Filippi, F. Vizza, J. Teddy, P. Serp and M. Zhiani. *J. Power Sources*, 190, 241, 2009.

[10] A. Kowal, S. Lj. Gojkovi´c, K-S- Lee, P. Olszewski, Y. –E. Sung. *Electrochem Communications*, 11, 724, 2009.

[11] Z. B. Wang, G. P. Yin, Y. G. Lin. *J. Power Sources*, 170, 242, 2007.

[12] R. Chetty, K. Scott. *Electrochim Acta*, 52, 4073, 2007.

[13] F. H. B. Lima, E. R. Gonzalez. *Electrochim Acta*, 53, 2963, 2008.

[14] T. Ioroi, T. Akita, S. Yamazaki, Z. Siroma, N. Fujiwara, K. Yasuda. *Electrochim Acta*, 52, 491, 2006.

[15] M. Zhu, G. Sun, Q. Xin. *Electrochim Acta*, 54, 1511, 2009.

[16] J.F.E. Gootzen, W. Visscher, J.A.R. Van Veen, *Langmuir*, 12, 5076, 1996.

[17] S.C.S. Lai, S.E.F. Kleyn, V. Rosca, M.T.M. Koper. *J. Phys. Chem. C*, 112, 19080, 2008.

[18] J.P.I. de Souza, S.L. Queiroz, K. Bergamaski, E.R. González, F.C. Nart. *J. Phys. Chem. B*, 106, 9825, 2002.

[19] C. Cremers, D. Bayer, B. Kintzel, M. Joos, F. Jung, M. Krausa, J. Tübke. *ECS Transactions*, 16, 1263, 2008.

[20] M.H. Shao, R.R. Adzic. *Electrochim Acta*, 50, 2415 2005.

[21] F. Colmati, G. Tremiliosi-Filho, E.R. González, A. Berna, E. Herrero, J.M. Feliu. *Faraday Discuss*, 140, 379, 2008.

[22] F. Hu, G. Cui, Z. Wei, P.K. Shen. *Electrochem Communications*, 10, 1303, 2008.

[23] L.G.S. Pereira, F.R. dos Santos, M.E. Pereira, V.A. Paganin, E.A. Ticianelli. *Electrochim Acta*, 51, 4061, 2006.

[24] F. Maillard, E. Peyrelade, Y. Soldo-Olivier, M. Chatenet, E. Chaînet, R. Faure. *Electrochim Acta*, 52, 1958, 2007.

[25] L.X. Yang, C. Bock, B. MacDougall, J. Park. *J. Appl. Electrochem*, 34, 427, 2004.

[26] P. Roquero. L.C. Ordóñez, O. Herrera, O. Ugalde, J. Ramírez. *Int. J. Chem. Reactor Eng*., 5, A99, 2007.

[27] A.C.C. Tseung, K.Y. Chen. *Catalysis Tod*ay, 38, 439, 1997.

[28] L. C. Ordóñez, P. Roquero, P.J. Sebastián, J. Ramírez. *Catalysis today*, 107-108, 46, 2005.

[29] G. Longini, P. Chini, *J. Am. Chem. Soc*, 98 (23), 10, 1976.

[30] W.H. Lizcano-Valbuena, V.A. Paganin, C.A.P. Leite, F. Galembeck, E.R.Gonzalez. *Electrochim Acta*, 48, 3869, 2003.

[31] Y. Takasu, T. Kawaguchi, W. Sugimoto, Y. Murakami. *Electrochim Acta*, 48, 3861, 2003.

[32] A. Stoyanova, V. Naidenov, K. Petrov, I. Nikolov, T. Vitanov, E. Budevski, *J. Appl. Electrochem*, 29, 1197, 1999.

[33] H. Razmi, Es. Habibi, H. Heidari. *Electrochim Acta*, 53, 8178, 2008.

[34] B. Bozzini, G. P. De Gaudenzi, B. Busson, C. Humbert, C. Six, A. Gayral, A. Tadjeddine. *J. Power Sources*, 195, 4119, 2010.

[35] E. Antolini. *J. Power Sources*, 170, 1, 2007.

[36] J. Melke, A. Schoekel, D. Dixxon, C. Cremers, D. Ramaker, C. Roth. *J. Phys. Chem. C*, 114, 5914, 2010.

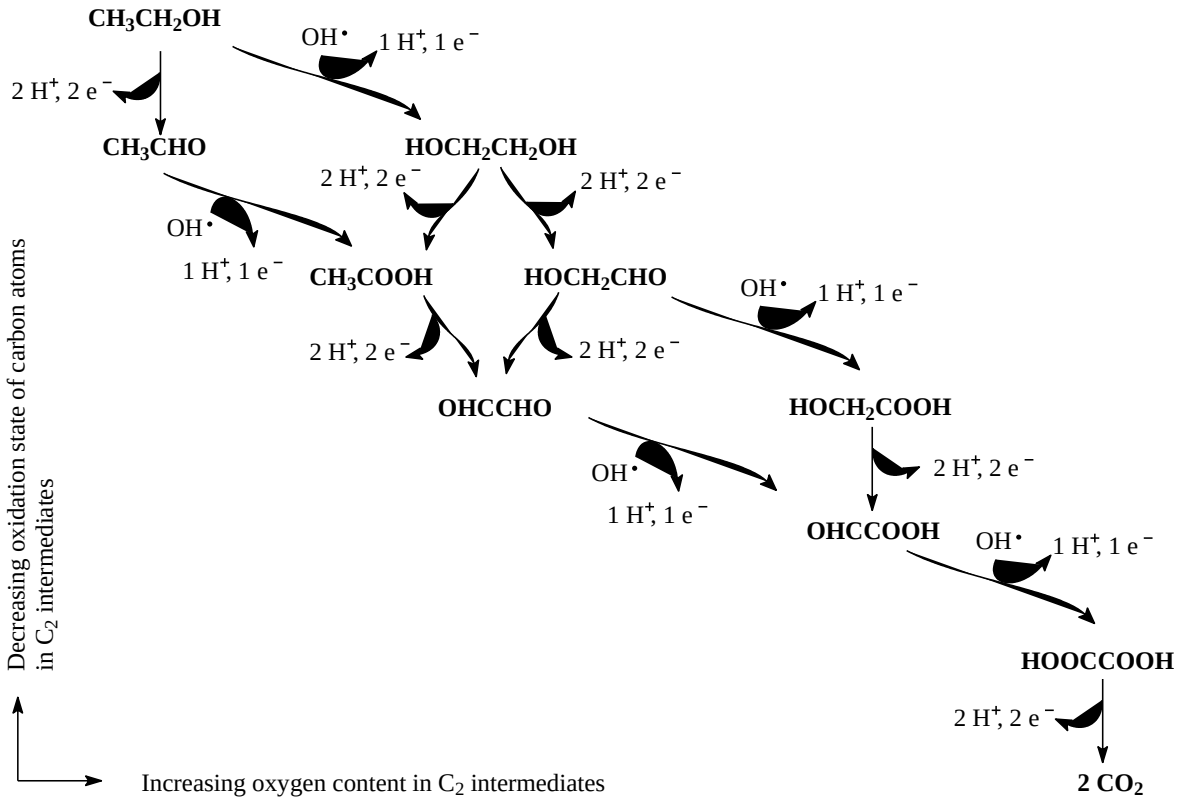

Scheme 1. Possible reaction pathways of ethanol oxidation toward CO_2, considering only stable C_2 intermediates.

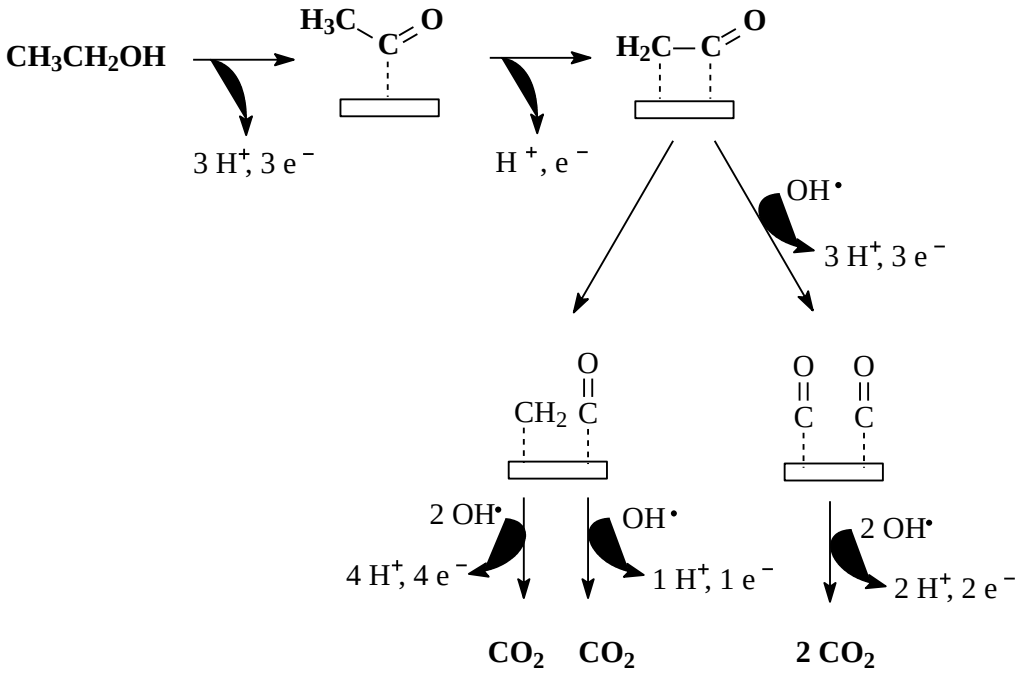

Scheme 2. Reaction pathways of ethanol oxidation toward CO_2, considering C_1 intermediates adsorbed at the catalyst active sites.

Table 1. Prepared materials.

Catalyst	**Weight %**			**Pt:W atomic ratio**
	Pt	**W**	**C**	
Pt_{20}/C_{80}	20	0	80	1:0
$Pt_{80}W_{20}/C$	20	5	75	4:1
$Pt_{67}W_{33}/C$	20	10	70	7:3
$Pt_{50}W_{50}/C$	20	20	60	1:1
W_{20}/C_{80}	0	20	80	0:1

Table 2. Results of the CO stripping voltammetry.

Catalyst	**Q** (mC)	$\mathbf{E_{onset}}$ (V vs SCE)	$\mathbf{E_{peak}}$ (V vs SCE)	$\mathbf{I_{peak}}$ (μA)	**Active area** (m^2/g cat)
Pt/C	4.452	0.3638	0.505	554.6	**4.23**
$Pt_{80}W_{20}/C$	3.714	0.3388	0.47857	414	**3.48**
$Pt_{67}W_{33}/C$	2.887	0.3528	0.4873	314.2	**2.70**
$Pt_{50}W_{50}/C$	2.524	0.402	0.520	258.1	**2.36**

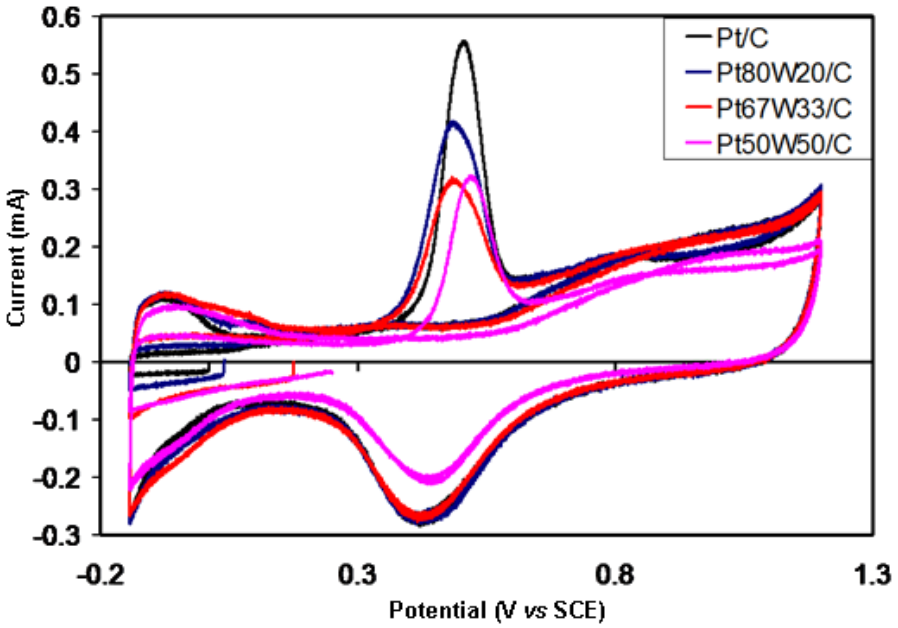

Figure 1. CO stripping voltammetry results from Pt-containing catalysts.

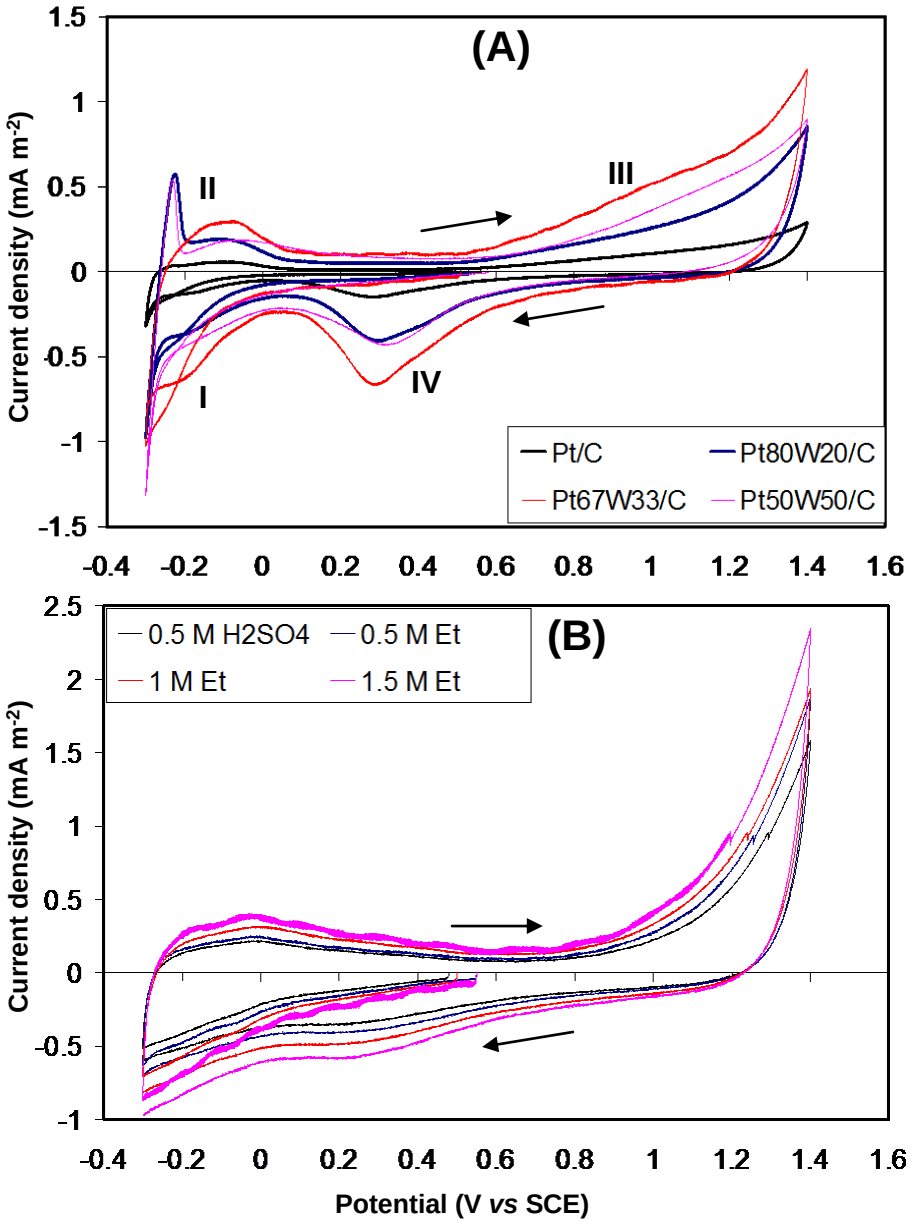

Figure 2. Cyclic voltammetry characterization in 0.5 M H_2SO_4. A: Pt catalysts; B: W_{20}/C_{80} material in sulfuric acid and different ethanol concentrations. Voltammograms recorded at 10 mV s^{-1}.

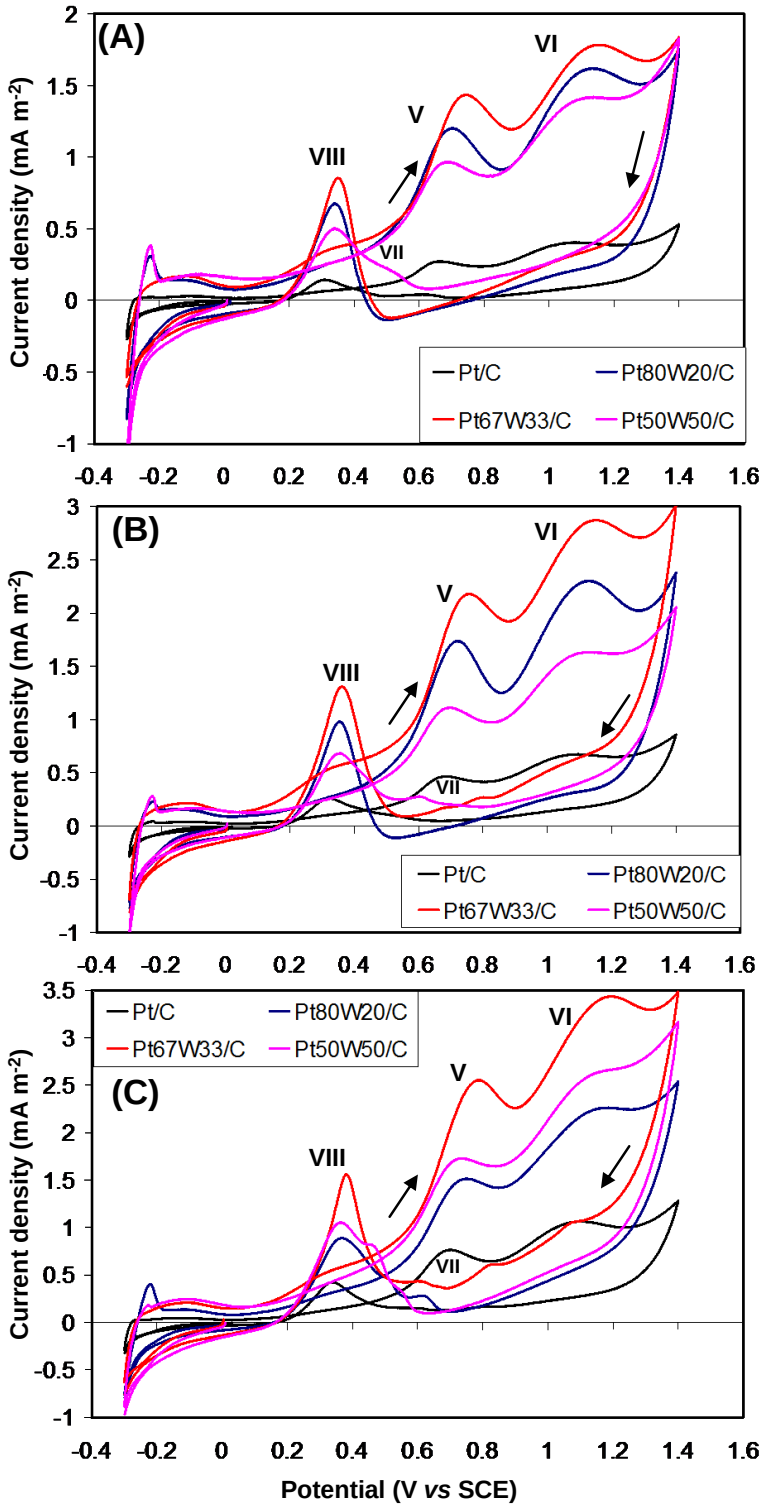

Figure 3. Cyclic voltammetry characterization of Pt catalysts in 0.5 M H_2SO_4. A: 0.5 M ethanol; B: 1 M ; C: 1.5 M. Voltammograms recorded at 10 mV s^{-1}.

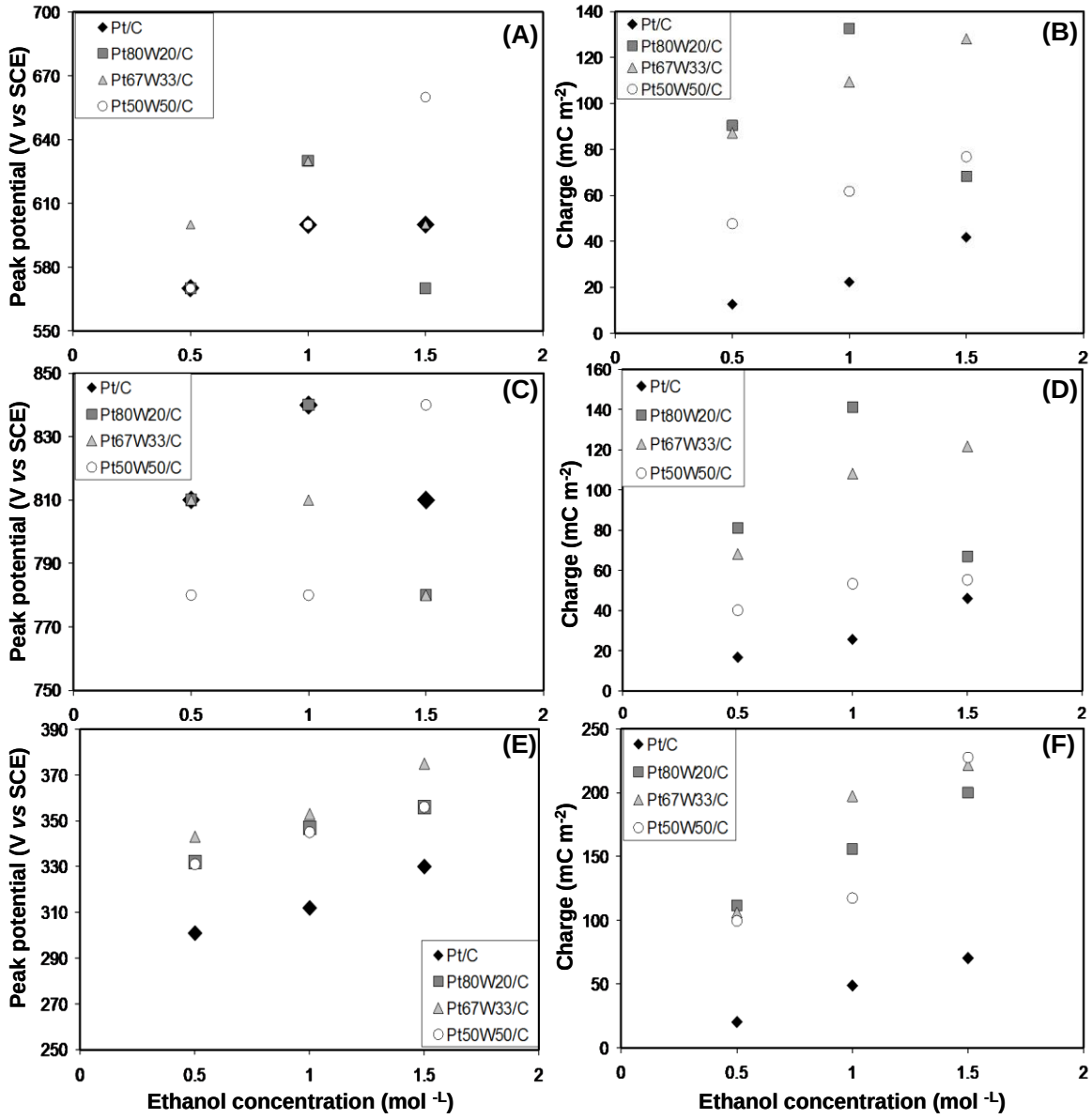

Figure 4. Peak potential and charge as a function of ethanol concentration, obtained at 50 mV s^{-1}. A,B: peak V; C,D: peak VI; E,F: peak VIII.

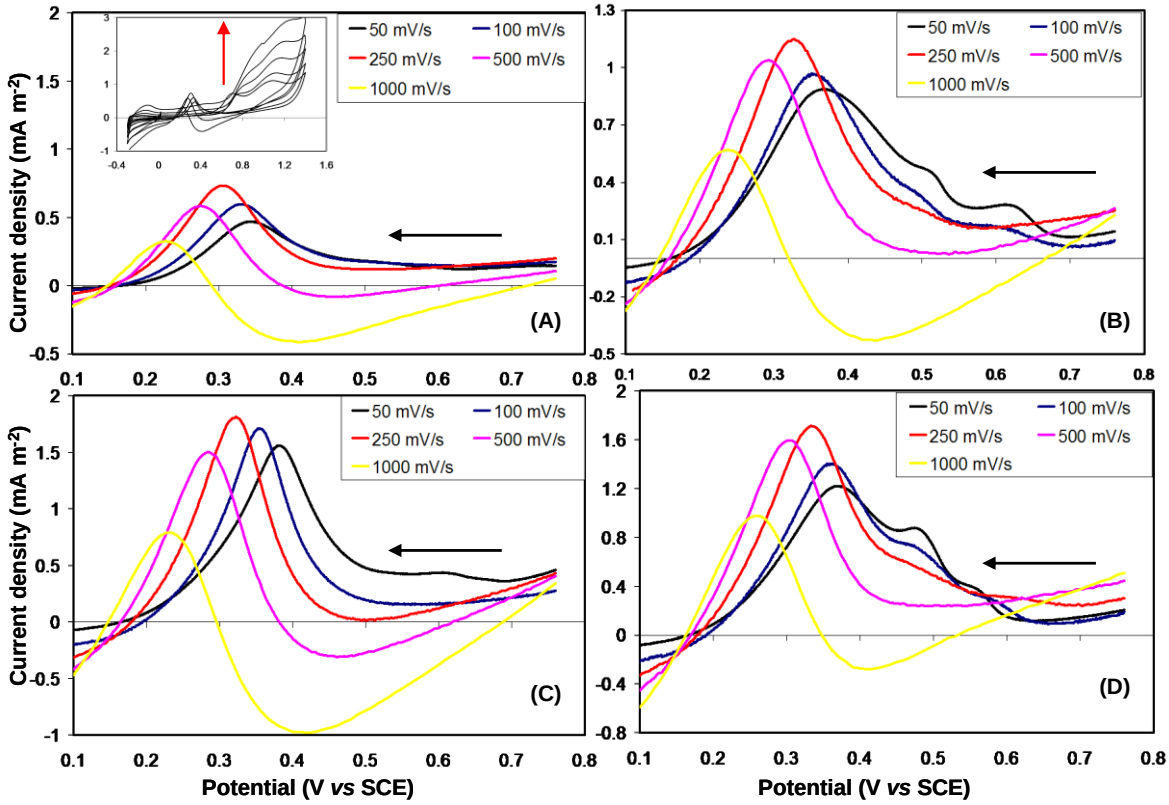

Figure 5. Voltammograms in negative-going potential sweeps at high scan rates in 0.5 M ethanol 0.5 M H_2SO_4. A: Pt_{20}/C_{80}; B: $Pt_{80}W_{20}/C$; C:$Pt_{67}W_{33}/C$; D: $Pt_{50}W_{50}/C$.

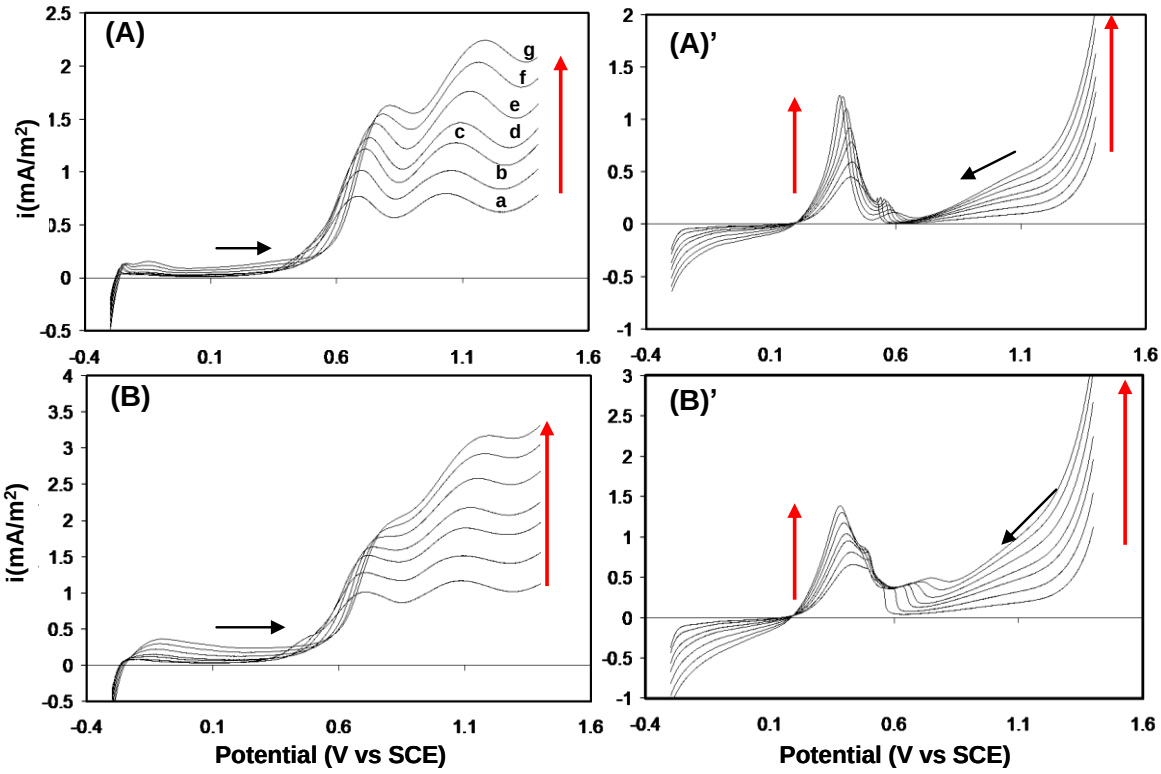

Figure 6. Cyclic voltammograms obtained in 0.5 M ethanol 0.5 M H_2SO_4. with variying scan rates. A: Pt_{20}/C_{80} positive – going sweep; A': Pt_{20}/C_{80} negative – going sweep; B: $Pt_{50}W_{50}/C$ positive – going sweep; B': $Pt_{50}W_{50}/C$ negative – going sweep. Black arrows indicate the scan direction. Red arrows indicate increasing scan rate: *a* to *g*: 5, 10, 20, 30, 50, 75, 100 mV s^{-1}, respectively.

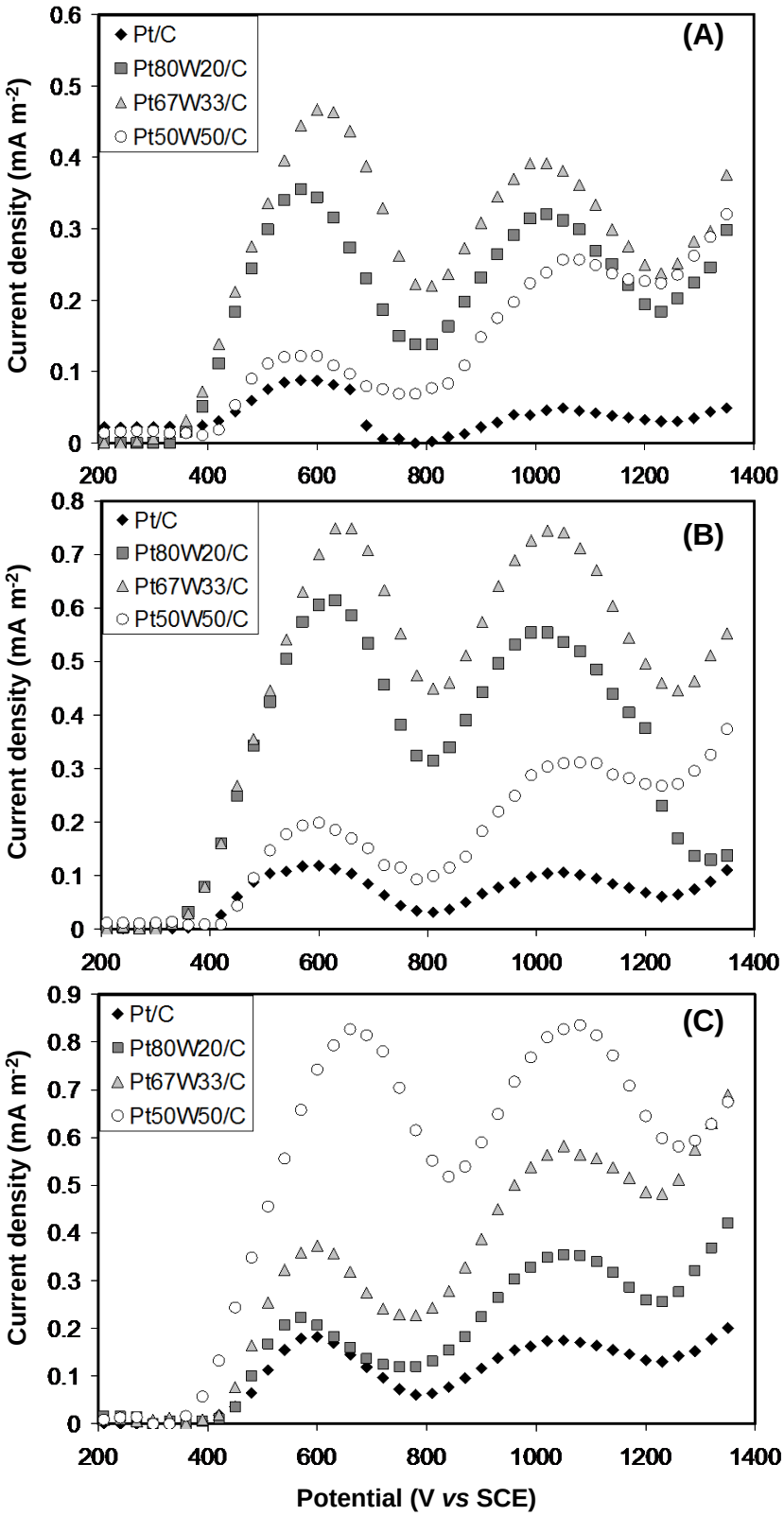

Figure 7. Current-sampled voltammetry results in 0.5 M H_2SO_4 and different ethanol, conentrations: A: 0.5 M; B:1 M; C:1.5 M.

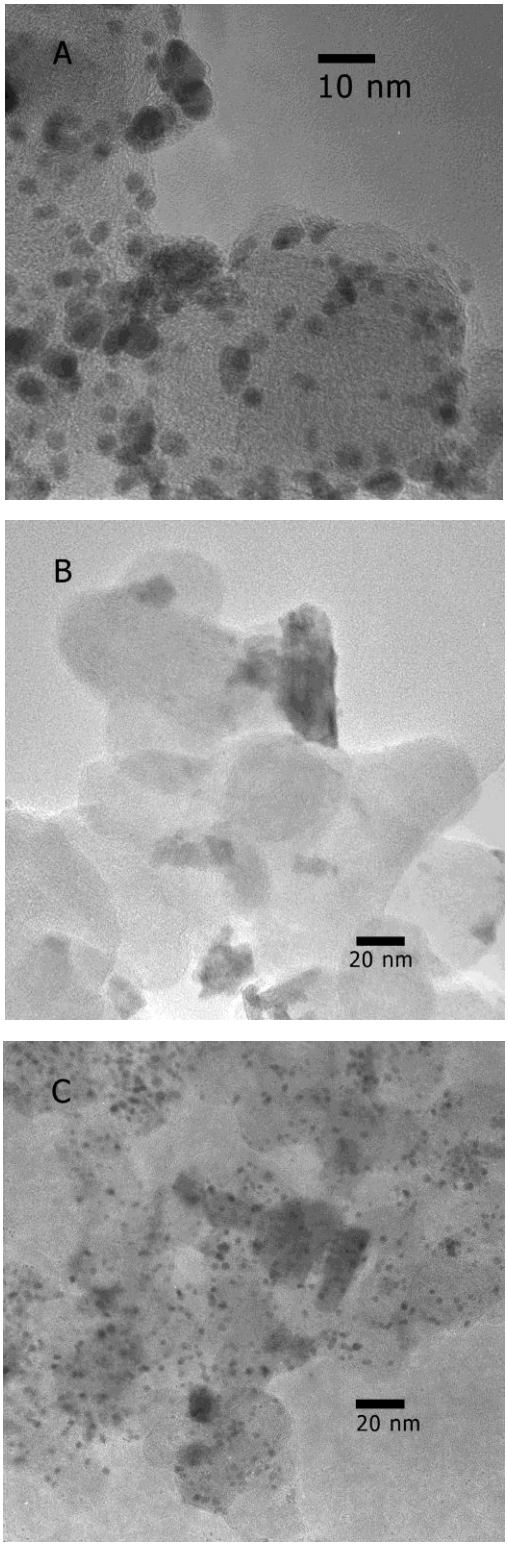

Figure 8. HRTEM microscopy images of A: Pt_{20}/C_{80} ; B: W_{20}/C_{80} ; C: $Pt_{50}W_{50}/C$